HCV revealed that expression of the interferon-stimulated genes (ISGs) was the principal reaction during the course of the viral infection and its clearance [5].

Type I IFNs are represented by the leukocyte and fibroblast types [6]. IFN-beta is encoded by a single gene, whereas IFN-alpha is represented by a large family of structurally related genes expressing 13 subtypes [7–10]. Among 13 proteins produced from these genes, IFN-alpha13 is identical to that produced from IFN-alpha1 gene. Thus, there are 12 different human IFN-alpha proteins. Several studies have shown that IFN-alpha subtypes have different properties in their mode of expression and the effects on the target cells depending on the cell types and on the IFN inducer used. In response to virus infection to murine cells, expression of IFN-alpha1, -alpha4, and -alpha6 mRNA are induced differently between cell types [11]. An analysis of mRNA expression in liver of chronic hepatitis C patients has shown that the expression patterns of each IFN subtype are different from those of normal controls [12].

In addition to the difference of the expression profile, IFN-alpha subtypes show different biological activities on their target cells. Each IFN-alpha subtype shows distinct patterns of antiviral, growth inhibitory, and other biologic activities [13–16]. Regarding antiviral activity, studies using murine encephalomyelitis virus and various human cell lines have shown that IFN-alpha8 was the most potent, while IFN-alpha1 was the least potent [17]. These reports have made us speculate that there might be subtype-specific IFN-signaling pathways.

Actions of type I IFN are initiated by binding of the IFN-alpha receptors (IFNARs) expressed on cell surface. The binding of IFN to their receptor activates two kinases; janus kinase 1 (JAK1) and the tyrosine kinase 2 (TyK2), which associate with the intracellular domain of IFNARs). These receptor-kinases activate the SH2 domain of the signal transducer and activator transcription factors (STATs). The phosphorylated STAT1 and STAT2 recruit IFN regulatory factor (IRF)-9 to form the IFN-stimulated gene factor-3 (ISGF-3) and activates expression of the ISGs by binding the interferon stimulation response element (ISRE) in their promoter/enhancer domain [18,19].

Studies on HCV replication have been hampered by the lack of efficient cell culture models. The problem was partly overcome by the development of an HCV subgenomic replicon system, which simulates cellular autonomous replication of HCV genomic RNA [20]. More recently, an efficient HCV cell culture system has been reported [21]. Replication of HCV replicon can be abolished by treatment with type I and type II IFNs [22–24]. These findings indicate that the IFN receptor-mediated cellular responses are intact in the HCV replicon system. In the present study, we have analyzed effects of five IFN-alpha subtypes on intracellular HCV replication using HCV subgenomic replicon system, and investigated on the difference of mechanisms of action.

2. Materials and methods

2.1. Cell culture

Huh7 and HeLa cells were maintained in Dulbecco's modified minimal essential medium (Sigma, St. Louis, MO) supplemented with 2 mM L-glutamine and 10% fetal calf serum at 37 °C under 5% CO_2. Huh7 cells containing HCV replicon were cultured in medium containing 500 μg/ml G418 (Nakalai, Kyoto, Japan).

2.2. HCV replicon constructs and transfected cell lines

An HCV subgenomic replicon plasmid, pHCVIbneo-delS was derived from an infectious HCV clone, HCV-N, genotype 1b [24]. The replicon was reconstructed by substituting the neomycin phosphotransferase gene with a fusion gene comprising the firefly luciferase and neomycin phosphotransferase (pRep-Feo) [25,26]. Another replicon construct, pSGR-JFH1 was derived from an infectious HCV clone, JFH-1, genotype 2a [27]. The replicon was reconstructed by substituting neomycin phosphotransferase gene with a fusion gene comprising of renilla luciferase and neomycin phosphotransferase (pRep-Reo). RNA was synthesized from linearized replicon plasmids using T7-polymerase (Promega, Madison, WI) and transfected into HeLa cells. After culture in the presence of G418, cell lines stably expressing the replicon were established (Huh7/Rep-Feo and HeLa/Rep-Reo). The expression levels of the replicon in the cell lines were determined by measuring luciferase activities of the cell lysates.

2.3. Reporter plasmids

A plasmid, pISRE-TA-Luc (BD Biosciences Clontech, Palo Alto, CA), expressed the Fluc gene under the control of the ISRE [28]. pGAS-TA-Luc, pAP1-TA-Luc, NF-kappa B-TA-Luc pSRE-TAL-luc, and pCRE-TAL-luc (BD Biosciences Clontech) are also used to see the expressed Fluc gene under GAS, AP1, NF-kappa B, SRE and CRE. A plasmid, pRL-CMV (Promega), which expresses the renilla luciferase gene under the control of the cytomegalovirus early promoter/enhancer, was used to normalize transfection efficiency.

2.4. Recombinant IFN-alpha subtypes

Recombinant human IFN-alpha1, -alpha2, -alpha5, -alpha8, and -alpha10 were prepared via the pET-3a-BL21 system (Novagen, Madison, WI) as described previously [29]. IFN-alpha activities were measured in a cytopathic effect (CPE) reduction assay using Sindbis virus-infected FL cells, and the IFN titers were standardizes in international units (IU/ml) by comparison with the WHO standard [29]. Cells were seeded in 96-well plates and incubated with two-fold dilutions of each IFN-alpha subtype. After incubation for 72 h, The CPE in each well was determined, and the specific

antiviral activity was expressed in terms of the mean 50% inhibitory concentration (IC50) of each IFN-alpha subtype on a weight basis. The activities were 3.0×10^6 IU/mg for subtype alpha1, 7.2×10^7 IU/mg for alpha2, 4.0×10^7 IU/mg for alpha5, 2.9×10^8 IU/mg for alpha8, and 4.9×10^7 IU/mg for alpha10. As regards IFN-alpha2, because of glycosylation of the naturally occurring subtype that may influence its biologic activity, we also purified natural IFN-alpha2 from cultures of BALL-1 cells stimulated with Sendai virus instead of producing a recombinant product. Recombinant interferon-alpha con1 was kindly provided by Yamanouchi Co. Ltd. (Tokyo, Japan). Specific activity of IFN-alpha con1 was 2.05×10^9 IU/mg [30].

2.5. Luciferase assays

Luciferase assays were done as described previously [28,31]. Typically, the replicon-expressing cells were seeded on a 24-well plate at a density of 1×10^4 cells per well. IFNs were applied to the culture medium at various concentrations (0.01–100 IU/ml). After 48 h of culture, expression levels of HCV replicon were measured by luciferase assay using the Bright-Glo Luciferase Assay System (Promega) or the Renilla Luciferase Assay System (Promega) and a luminometer, TD-20/20 (Turner Designs, Sunnyvale, CA). Assays were done in triplicate and the results were expressed as means ± S.D. To perform dual reporter assays, cells were seeded onto 24-well plate at 5×10^4 cells per well, and transfected with 400 ng of pISRE-TA-Luc and pRL-CMV(1 ng for Huh7, 10 ng for HeLa, respectively) using 1.2 μl of FuGene6 (Roche, Indianapolis, IN) per well. IFN-alpha subtypes were applied at 24 h after the transfection. Cells were harvested at 24 h after the addition of IFNs. The dual reporter assays were done using the Dual-Luciferase Reporter Assay System (Promega).

2.6. Western blot analysis

Ten micrograms of nuclear extract lysate was separated in a NuPAGE 10% Bis–Tris Gel (Invitrogen) and blotted onto the PVDF Western Blotting Membrane (Roche). The membranes were incubated with mouse monoclonal anti-NS5A antibody followed by POD-labeled anti-mouse IgG antibody. Chemiluminescence was detected using the ECL Western blotting Analysis System (Amersham Biosciences, Buckinghamshire, UK) according to the manufacturer's protocol.

2.7. Analyses of drug synergism

The effects of treatment of Huh7/Rep-Feo cells with the IFN subtypes, alone and in combination, were analyzed according to classical isobologram analysis [32,33]. Dose–inhibition curves of IFN subtypes A and B were drawn, with the two drugs used alone or in combination. In each drug combination, the concentrations of IFN subtypes A and B that inhibited HCV replication to 50% (IC50) were plotted against the fractional concentration of each IFN subtype on the *X*- and *Y*-axes, respectively. The combination index, CI, for each combination was calculated using the following formula:

$$CI = \frac{IC50(\text{IFN subtypes A and B combined})}{IC50\,(\text{IFN subtype A alone})} + \frac{IC50(\text{IFN subtypes A and B combined})}{IC50\,(\text{IFN subtype B alone})}$$

For such plots, the combined effects of two drugs can be assessed as an either additive effect, indicated by $CI = 1$, synergy, indicated by $CI < 1$, or antagonism, indicated as $CI > 1$.

2.8. Reverse transcription-polymerase chain reaction (RT-PCR) assay

Total cellular RNA was extracted from cells using ISOGEN (Wako, Osaka, Japan). Two micrograms of total cellular RNA was used to synthesize cDNA from each sample using the SuperScript II (Invitrogen) reverse transcriptase. PCR was done in a mixture containing 1 μl cDNA sample; 1.25 mM $MgCl_2$; 0.5 μM of each primer; 0.4 mM of dNTP and BD advantage2 PCR Kit (BD Biosciences Clontech, Palo Alto, CA). Primers used were as follows: IFNAR-1, sense, 5′-AGT GTT ATG TGG GCT TTG GAT GGT TTA AGC-3′, IFNAR-1, antisense, 5′-TCT GGC TTT CAC ACA ATA TAC AGT CAG TGG-3′, IFNAR-2, sense, 5′-ATT TCC ATC TAT TGT TGA GG-3′, IFNAR-2, antisense, 5′-CAC TTT CTT CTT TCT GTT GA-3′, beta-actin, sense, 5′-CAC CAT GGA TGA TGA TAT CGC CGC GCT CGT-3′, and beta-actin, antisense, 5′-GAA GCA TTT GCG GTG GAC GAT GGA GGG GCC-3′. The PCR products were separated on 1% agarose gel, stained with etidium bromide, and visualized by UV transilluminator.

2.9. Statistical analyses

Statistical analyses were performed using the Student's *t*-test; *p*-values of less than 0.05 were considered as statistically significant.

3. Results

3.1. Analysis of suppressive effects of the IFN-alpha subtypes on expression of HCV replicon in Huh7 cells

Huh7/Rep-Feo cells were treated with various concentrations of IFN subtypes (0.01–100 IU/ml). After 48 h of the treatment, the levels of HCV replication were analyzed by luciferase assay. Replication level of HCV replicon was significantly suppressed by each IFN subtype in dose-dependent manner (Fig. 1A). Fifty percent inhibitory concentrations (IC50) of the IFN subtypes were calculated as 0.375 IU/ml (125 pg/ml) for alpha1, 0.220 IU/ml (3.05 pg/ml) for alpha2, 0.238 IU/ml (5.94 pg/ml) for alpha5, 0.124 IU/ml

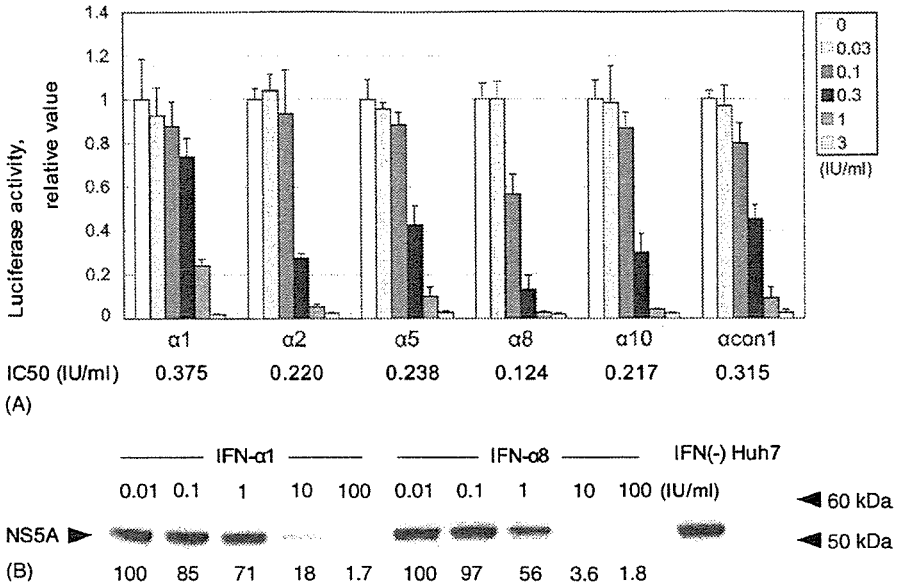

Fig. 1. Analysis of antiviral effect of the IFN-alpha subtypes using HCV replicon Huh7 cells: (A) luciferase activities of Huh/Rep-Feo were cultured in the presence of indicated concentration of IFN subtypes. Luciferase activities were measured at 48 h after culture. Values indicate relative luciferase activities as percents of IFN-negative controls. Error bars indicate mean ± S.D. (B) Western blotting. Huh7/Rep-Feo cells were treated with indicated concentrations (numbers on the top) of IFN-alpha1 and -alpha8. Total cell lysate was harvested after 48 h, and Western blotting was done using primary antibody directed against NS5A. Numbers on the bottom indicate densitometric values displayed as percents of an IFN-negative control.

(0.429 pg/ml) for alpha8, 0.217 IU/ml (4.43 pg/ml) for alpha10, and 0.315 IU/ml (0.153 pg/ml) for alpha con1, respectively. As indicated, expression of HCV replicon in Huh7 cells was the most sensitive to IFN-alpha8, and the least to IFN-alpha1 by titers standardized in IU/ml and in pg/ml. IFN-alpha8 was 1.8 times more sensitive than IFN-alpha2 to suppress HCV replication. Treatment of Huh7/Rep-Feo with a solvent of IFN proteins showed no effects on expression levels of HCV replicon. To confirm the result of IFN-alpha1 and -alpha8, we next carried out Western blotting. Cells were treated with IFN-alpha1 and -alpha8, and total cell lysate was harvested after 48 h. The expression of replicon-derived NS5A protein was dose-dependently suppressed by treatment with IFN-alpha1 and -alpha8, and the velocities of suppression were comparable to those of luciferase activities (Fig. 1B).

3.2. *Effects of IFN subtypes on cellular signal transduction pathways*

We next investigated effects of IFN subtypes on the ISRE and GAS promoter activities by luciferase reporter assay. Plasmids, pISRE-luc and pGAS-luc were transfected into Huh7 cells. Twenty-four hours after transfection, various concentrations of IFN subtypes were added into the medium. Luciferase assay was done at 6 h after addition of IFNs. The ISRE- and GAS-mediated luciferase activities were elevated by dose-dependent manner of each IFNs. However, there was no significant difference in their induction velocities between each IFN subtypes (Fig. 2A). Furthermore, a discrepancy was observed between the suppressive effects of HCV replication and the ISRE and GAS activities; IFN-alpha1 and -alpha8 apparently showed similar activations of ISRE and GAS promoter, while IFN-alpha8 was more effective to inhibit the HCV replication than IFN-alpha1. Therefore, we investigate alternate pathway that may be activated by IFN. Reporter assays were performed by using plasmids, pAP1-luc, pNF-kappa B-luc, pCRE-luc, and pSRE-luc. Luciferase assays after addition of each IFN subtypes showed that neither of AP1, NF-kappa B, CRE, and SRE reporters were activated by IFN treatment (Fig. 2B).

3.3. *Analyses of synergism between IFN subtypes*

It has been reported that interactions between IFN subtypes may influence cellular response to IFN [16]. Our previous study showed that IFN-alpha2 and -alpha8 had synergistic antiviral effect against vesicular stomatitis virus (VSV) infection to HepG2 cells. [29]. To investigate if the IFN subtypes synergistic effects on HCV replication, a classical isobologram analysis was performed [32,33]. Huh7/Rep-Feo cells were treated with IFN-alpha2 or -alpha8 alone, or with IFN-alpha2 and -alpha8 that were mixed with equivalent IC50 ratio, and the dose–effect plots were drown (Fig. 3A). Each concentration of IFN-alpha2 and -alpha8 at 50% inhibition were plotted on the *X*- and *Y*-axes, respectively, to generate an isobologram (Fig. 3B). A plot showing the IC50 of IFN-alpha2 and -alpha8 at 1:1 mixture was located on the line connecting IC50 of IFN-alpha2 or -alpha8 alone, indicating that the effects of the drug

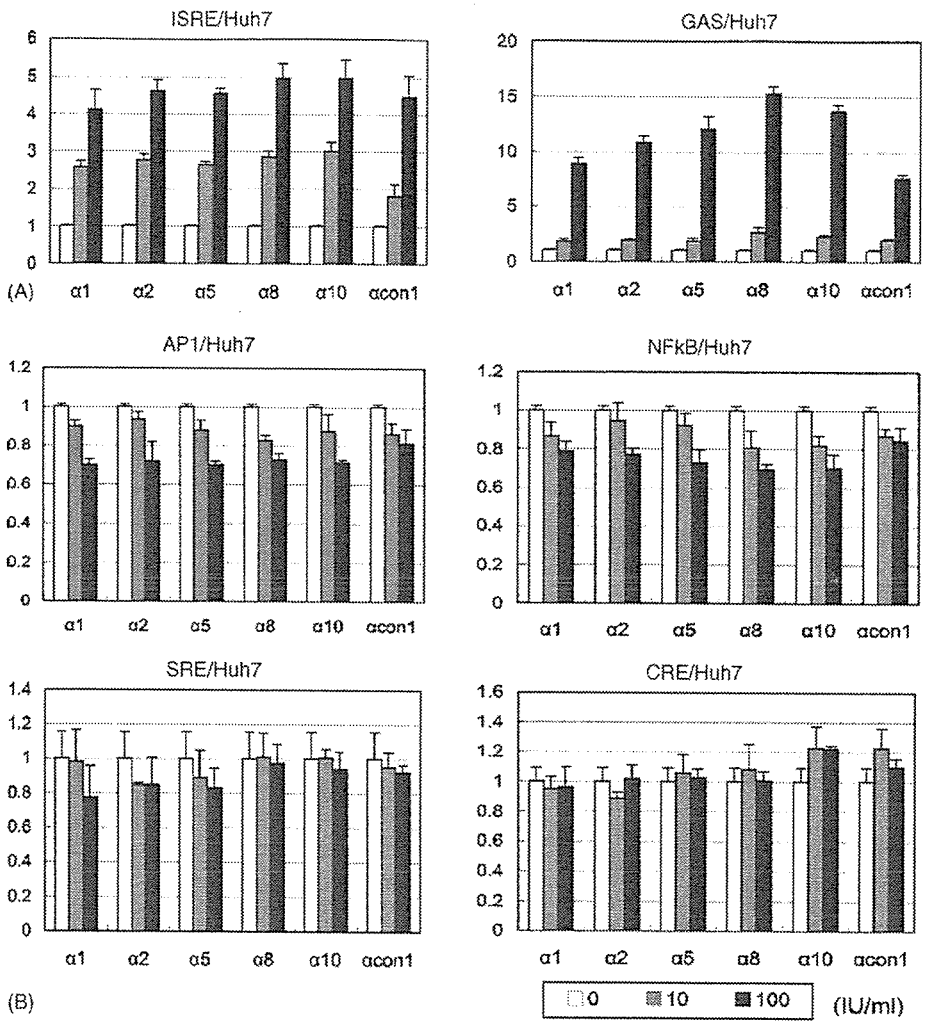

Fig. 2. ISRE, GAS, AP1, NF-kappa B, CRE and SRE reporter assay of Huh7 cells. ISRE-, GAS-, AP1-, NF-kappa B-, CRE-, or SRE-Luc reporter plasmids was transfected into Huh7 with pRL-CMV as a control. Twenty-four hours after transfection, the medium was supplemented with the IFN-alpha subtypes indicated. Dual luciferase assays were done at 6 h after the addition of IFNs. Bars indicate relative reporter activities as percents of IFN-negative controls. Error bars indicate mean ± S.D.

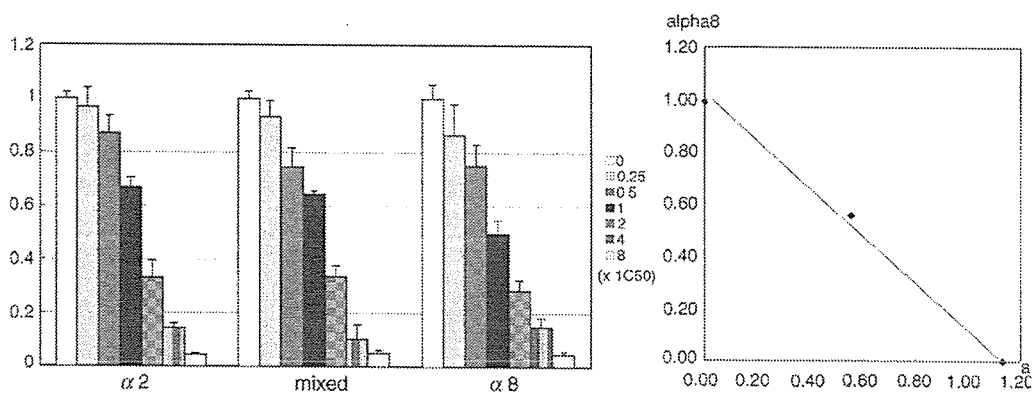

Fig. 3. Analyses of synergism between IFN subtypes 2 and 8: (A) IFNs; IFN-alpha2, -alpha8, mixed, dose modified by IC50 are added to Huh/Rep-Feo. Luciferase activities of Huh/Rep-Feo were measured 48 h after the addition of IFNs. (B) Graphical representation of the isobologram analysis. IC50s were calculated from the values in panel A. Each fractional IC50 for IFN-alpha2 and -alpha8 was plotted on *X*- and *Y*-axes, respectively. The FIC plot for the IFN-alpha2 and -alpha8 combinations of 1:1 falls on a theoretical line of additivity that is drawn between the IS50 plot for each IFN alone, indicating the effects of combination of IFN-alpha2 and -alpha8 is additive.

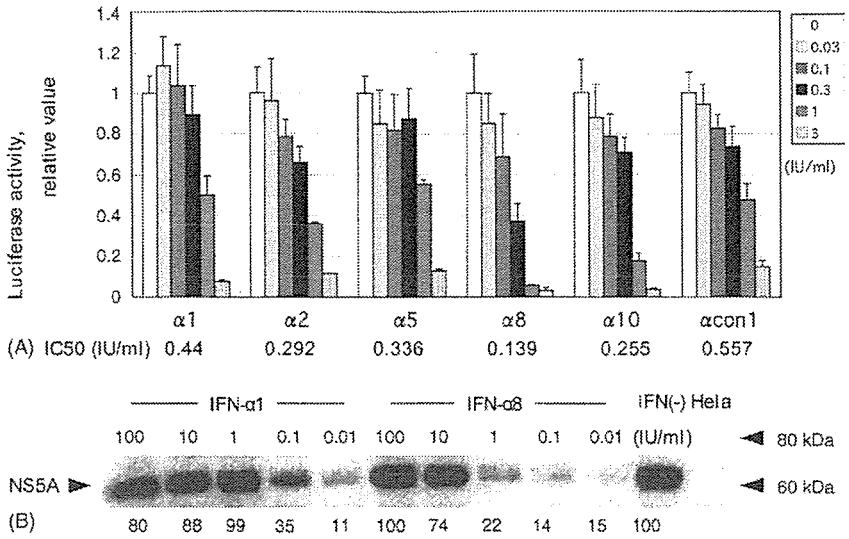

Fig. 4. Analysis of antiviral effect of the IFN-alpha subtypes using HCV replicon HeLa cells: (A) Luciferase activities of HeLa/Rep-Reo were cultured in the presence of indicated concentration of IFN subtypes. Luciferase activities were measured at 48 h after culture. Values indicate relative luciferase activities as percents of IFN-negative controls. Error bars indicate mean ± S.D. (B) Western blotting. HeLa/Rep-Reo cells were treated with indicated concentrations (numbers on the top) of IFN-alpha1 and -alpha8. Total cell lysate was harvested after 48 h, and Western blotting was done using primary antibody directed against NS5A. Numbers on the bottom indicate densitometric values displayed as percents of an IFN-negative control.

combination on intracellular HCV-RNA replication is additive.

3.4. Analysis of antiviral effect of the IFN-alpha subtypes using HCV replicon HeLa cells

Different type of cells may respond to IFN in a different manner possibly depending on the expression profiles of interferon receptors or cellular factors that mediate IFN signal transduction. To investigate the effects of IFN subtypes in a non-hepatocyte cell line, we used HeLa cells expressing chimeric luciferase reporter HCV replicon, HeLa/Rep-Reo. Treatment of HeLa/Rep-Reo cells with IFN subtypes suppressed expression of HCV replicon in dose-dependent manner (Fig. 4A). The IC50 for each IFN subtypes were 0.44 IU/ml (147 pg/ml) for alpha1, 0.292 IU/ml (4.06 pg/ml) for alpha2, 0.336 IU/ml (8.4 pg/ml) for alpha5, 0.139 IU/ml (0.479 pg/ml) for alpha8, 0.255 IU/ml (5.20 pg/ml) for

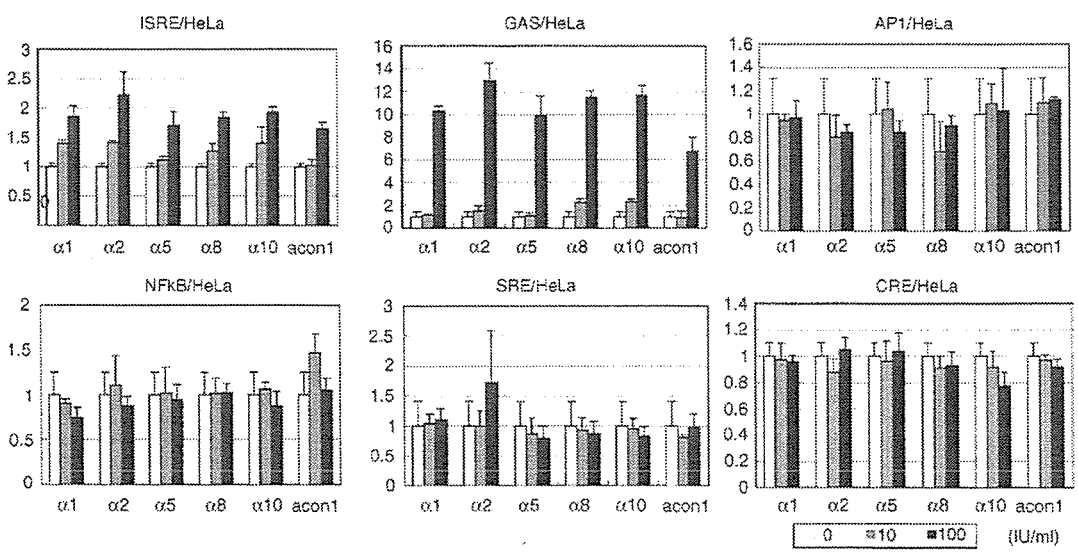

Fig. 5. Reporter assay of HeLa cells. ISRE-, GAS-, AP1-, NF-kappa B-, CRE-, and SRE-Luc reporter plasmids were, respectively, transfected into HeLa cells with pRL-CMV as a control. Twenty-four hours after transfection, IFN subtypes were added onto the medium. Dual luciferase assays were done at 6 h after the addition of IFNs. Bars indicate relative reporter activities as percents of IFN-negative controls. Error bars indicate mean ± S.D.

alpha10, and 0.557 IU/ml (0.271 pg/ml) for alpha con1, respectively. Similarly to the Huh7 cells, IFN-alpha8 was the strongest to suppress expression of HCV replicon. On the other hand, IFN-alpha5 and alpha con1 showed weaker antiviral effects on HCV replicon in HeLa cells than in Huh7 cells. Western blotting of HeLa/Rep-Reo cells treated with IFNs-alpha1 and alpha8 showed dose-dependent suppression of HCV replication, and differential activities of IFN subtypes, which were comparable to that of luciferase activities (Fig. 4B).

Reporter assays were performed by transfecting plasmids expressing ISRE-, GAS-, AP1-, NF-kappa B-, CRE-, and SRE-luciferase reporters into HeLa cells. The ISRE- and GAS-luciferase constructs responded to treatment with IFN subtypes similarly to that in Huh7 cells (Fig. 5). There was no significant difference in induction velocity of ISRE and GAS reporter activities between different IFN subtypes as were seen in Huh7 cells. IFN treatment showed no significant effects on AP1, NF-kappa B, CRE, and SRE activities on HeLa cells.

3.5. Analyses of IFN receptors expression

It is possible that the differences in expression levels of the cell-surface IFN receptors may associate with the response to IFN. We then analyzed expression of the respective subunits of type I IFN receptor mRNAs of Huh7 and HeLa cells by RT-PCR. Type I IFN receptor, IFNAR, is constituted by two subunits; 110 kilo-dalton (kDa) alpha subunit (IFNAR-1), and a 102 kDa beta subunit (IFNAR-2). IFNAR-2 has three isoforms that are translated from alternatively spliced mRNA transcripts; a 40 kDa soluble form of IFNAR-2a, a 55 kDa short form of IFNAR-2b and a 102 KDa long form of IFNAR-2c [34–36]; IFNAR-2c is the authentic beta subunit that is functionally active and coexpressed with IFNAR-1 (Fig. 6A). An RT-PCR analysis of IFN receptors showed that both cell lines expressed IFNAR-1 and IFNAR-2 (Fig. 6B). Although the relative expression levels of IFNAR-2a was slightly higher in Huh7 cells that in HeLa cells, There were no apparent differences in the expression level of the major subunits, IFNAR-1 and IFNAR-2c between Huh7 and HeLa cells.

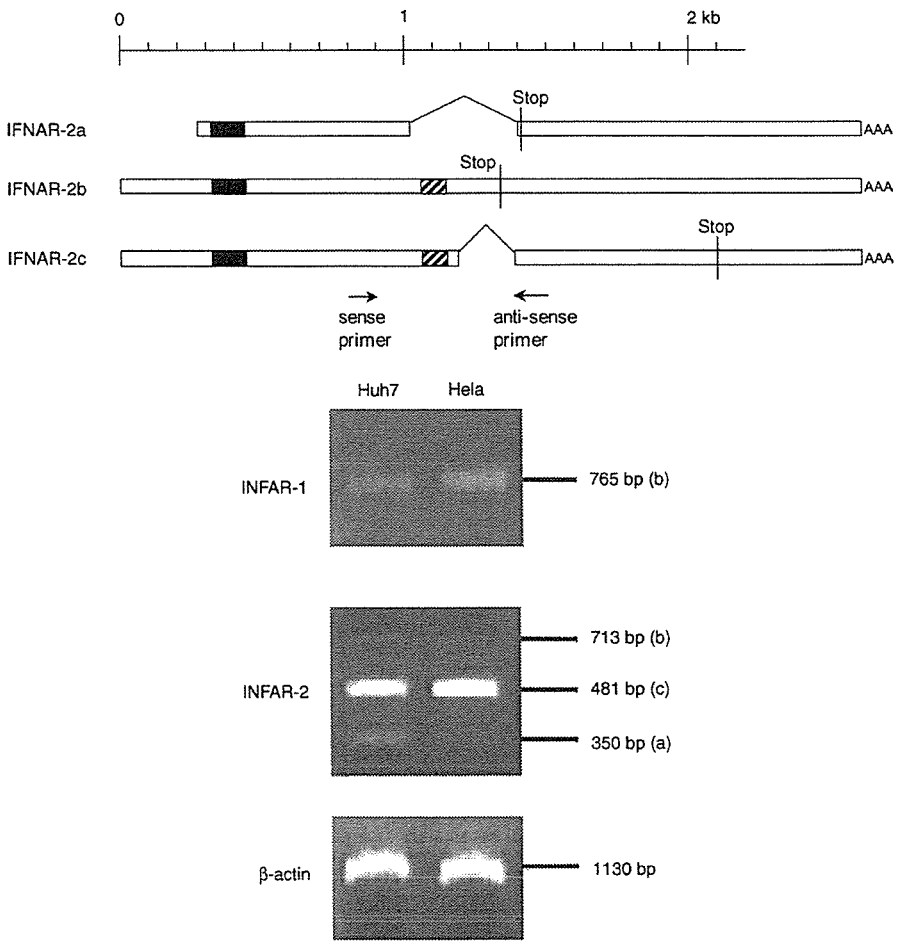

Fig. 6. IFN receptor expression: (A) structures of 3 IFNAR2 mRNA isoforms. Closed boxes indicate the leader peptide domains. The striped boxes indicate the transmembrane domain. Stop codons are indicated by vertical bars. Position of the sense and antisense primers are shown at the bottom. (B). Expression of IFN-alpha receptors in Huh7 and HeLa cells were evaluated by RT-PCR. The top panel: IFNAR-1 PCR-amplified DNA of 765 bp. The middle panel: IFNAR-2 PCR products, (a) 350 bp as IFNAR-2a, (b) 713 bp as IFNAR-2b, and (c) 481 bp as IFNAR-2c in size, respectively. The bottom panel: beta actin DNA.

4. Discussion

In this study, we used two cell lines that support expression of HCV replicon, in which the level of the viral genomic replication can by readily monitored by luciferase reporter assay. We showed that the five IFN-alpha subtypes have different activities to suppress expression of HCV replicon (Figs. 1 and 3). Using two IFN titers standardized in IU/ml and in pg/ml, IFN-alpha8 had the strongest antiviral effect on replicon, while IFN-alpha1 had the weakest effect in both titers. These finding are consistent with those reported by Foster et al. that IFN-alpha8 had the greatest antiviral activity in cells of three human tumor cell lines challenged with murine encephalomyelitis virus [17]. On the other hand, the reporter assay showed that activation of ISRE-dependent promoter, which is the primary signal transduction pathway, showed very similar results between Huh7 and HeLa cells, while the ISRE activities in neither of the cell lines correlated with the anti-HCV activities of the IFN subtypes (Figs. 2 and 4). GAS reporter activity, which bound by phosphorylated STAT1 homodimer, showed similar activation between each IFN subtypes. Other reporter assays, NF-kappa B, CRE, and SRE, showed no activation by the IFNs. These findings suggest that the divergent action of IFN subtypes may be independent of the classical JAK-STAT pathway.

Beside the classical JAK1-STAT1 and -2 pathway, type I IFN activates alternative signaling pathways. JAK2 mediates activity of IFNs as well as JAK1. As for STAT family, dimmers of STAT1:1, STAT3:3, STAT1:3, STAT5:5, and a heterodimer CrkL:STAT5 have been reported to be formed during the IFN-alpha signaling [18,19]. Furthermore, IFN-alpha treatment of cells activates expression of various genes that modulate virus infection and replication in JAK-STAT-independent manner; those include the insulin receptor substrate family, CrkL adaptor, protooncogene Vav, PKC-delta, p38 kinase, ERK 1/2, and PI-3 kinase, although the targets for these signaling pathways have not been well understood (reviewed in [18,19]).

Actions of IFN-alpha is initiated by binding the type I IFN receptors. It has been suggested that biologic activities of different IFN-alpha subtypes correlate with their respective binding affinities to the cells used [37]. Although we have not tested the cell-binding affinity of the IFN subtypes onto their receptor, activation of ISRE promoter, which is triggered by the receptor binding of IFN, did not correlate with their antiviral activities. Furthermore, analyses of IFN receptors by RT-PCR did not find differences in expression profiles the type I IFN receptor subunits, IFNAR1 and three isoforms of IFNAR2 [34–36] in Huh7 and HeLa cells that support expression of HCV replicon (Fig. 6B), suggesting that the differential effects of IFN subtypes may not be due to different expression profiles of their receptor subunits. Alternatively, binding of IFNs onto their receptor might recruit unidentified subunits or adaptor molecules that may activate aberrant signal transduction pathways.

Most studies on actions of the IFN subtypes focused only on the effects of the individual subtypes, and very little is known about their effects in combination [38–40]. On the other hand, because of the existence of multiple IFN subtypes, mutual interactions between the subtypes may be involved in the cellular responses, although these interaction between IFN subtypes are not well understood. Greiner et al. had reported IFN-alpha1 competes with IFN-alpha2 for binding to its receptor [16]. Our previous study also demonstrated additive and antagonistic effect of IFN-alpha subtypes, for instance, IFN-alpha2 and alpha8 had synergistic antiviral effect against VSV virus in HepG2 cells. [29] In our present study, we could not find such synergistic effects of IFN-alpha2 and alpha8 subtypes on cellular HCV replication (Fig. 3B). The result suggests that effects of IFN subtypes and their combination may show different effects depending on the target pathogens.

IFN-alpha con1 is a recombinant IFN that has consensus amino acid sequence of multiple IFN-alpha subtypes on its receptor-binding domain. The IFN-alpha con1 shows greater antiviral activity against HCV replication than the individual IFN-alpha subtypes in vitro [41] as well as in vivo [42]. In our present study, IFN con1 was moderately effective to suppress HCV replication with the IC50 of close to that of IFN-alpha5. However, activation of ISRE and GAS by IFN-alpha con1 seemed to be slight weaker, compared to the other IFN subtypes. Although it might be due to the different definition of units from that of the other IFN-alpha subtypes [30,41], the reportedly strong biological activity of IFN-alpha con1 might also involve pathway other than the Jak-STAT pathway.

Our present results using HCV replicon system have shown that IFN-alpha8 was the strongest to suppress HCV replication among 5 IFN-alpha subtypes 1, 2, 5, 8, and 10. Among clinically used IFN-alpha preparations, natural IFN-alpha preparations contain substantial amounts of IFN-alpha8 [29]. The differential activity shown in this study might direct a spotlight to the drugs, and might propose a hint for more effective IFN drugs used alone or in combination with ribavirin. Taken togather, IFN-alpha8 showed the strongest suppressive effect on in vitro HCV replication. The discrepancy between cellular ISRE responses and the anti-HCV effect implies other pathways other than IFN-activated JAK-STAT pathway. Further investigation of their differential antiviral actions may help elucidating the IFN-mediated cellular defense mechanisms against virus infection.

Acknowledgements

We are indebted to Dr. Takaji Wakita for providing a replicon construct, pSGR-JFH1. A part of this study was partly supported by a grants from Ministry of Education, Culture, Sports, Science and Technology of Japan (17015014), and by grants from Japan Society for the Promotion of Science (17590626).

References

[1] Alter MJ. Epidemiology of hepatitis C. Hepatology 1997;26:62S–5S.
[2] Fried MW, Shiffman ML, Reddy KR, et al. Peginterferon alfa-2a plus ribavirin for chronic hepatitis C virus infection. N Engl J Med 2002;347:975–82.
[3] Samuel CE. Antiviral actions of interferons. Clin Microbiol Rev 2001;14:778–809.
[4] Taniguchi T, Takaoka A. The interferon-alpha/beta system in antiviral responses: a multimodal machinery of gene regulation by the IRF family of transcription factors. Curr Opin Immunol 2002;14:111–6.
[5] Bigger CBBKM, Lanford RE. DNA microarray analysis of chimpanzee liver during acute resolving hepatitis C virus infection. J Virol 2001;75:7059–66.
[6] Pestka S, Baron S. Definition and classification of the interferons. Methods Enzymol 1981;78:3–14.
[7] Nagata S, Taira H, Hall A, et al. Synthesis in E. coli of a polypeptide with human leukocyte interferon activity. Nature 1980;284:316–20.
[8] Hobb DS, Moschera JA, Levy WP, Pestka S. Purification of interferon produced in a culture of human granulocytes. Methods Enzymol 1981;78:472–81.
[9] Henco K, Brosius J, Fujisawa A, et al. Structural relationship of human interferon alpha genes and pseudogenes. J Mol Biol 1985;185:227–60.
[10] Diaz MO, Bohlander S, Allen G. Nomenclature of the human interferon genes. J Interferon Cytokine Res 1996;16:179–80.
[11] Bisat F, Raj NB, Pitha PM. Differential and cell type specific expression of murine alpha-interferon genes is regulated on the transcriptional level. Nucleic Acids Res 1988;16:6067–83.
[12] Castelruiz Y, Larrea E, Boya P, Civeira MP, Prieto J. Interferon alfa subtypes and levels of type I interferons in the liver and peripheral mononuclear cells in patients with chronic hepatitis C and controls. Hepatology 1999;29:1900–4.
[13] Evinger M, Rubinstein M, Pestka S. Antiproliferative and antiviral activities of human leukocyte interferons. Arch Biochem Biophys 1981;210:319–29.
[14] Fish EN, Banerjee K, Stebbing N. Human leukocyte interferon subtypes have different antiproliferative and antiviral activities on human cells. Biochem Biophys Res Commun 1983;112:537–46.
[15] Ortaldo JR, Herberman RB, Harvey C, et al. A species of human alpha interferon that lacks the ability to boost human natural killer activity. Proc Natl Acad Sci USA 1984;81:4926–9.
[16] Greiner JW, Fisher PB, Pestka S, Schlom J. Differential effects of recombinant human leukocyte interferons on cell surface antigen expression. Cancer Res 1986;46:4984–90.
[17] Foster GR, Rodrigues O, Ghouze F, et al. Different relative activities of human cell-derived interferon-alpha subtypes: IFN-alpha 8 has very high antiviral potency. J Interferon Cytokine Res 1996;16:1027–33.
[18] Uddin S, Platanias LC. Mechanisms of Type-I interferon signal transduction. J Biochem Mol Biol 2004;37:635–41.
[19] Caraglia M, Marra M, Pelaia G, et al. Alpha-interferon and its effects on signal transduction pathways. J Cell Physiol 2005;202:323–35.
[20] Lohmann V, Korner F, Koch J, Herian U, Theilmann L, Bartenschlager R. Replication of subgenomic hepatitis C virus RNAs in a hepatoma cell line. Science 1999;285:110–3.
[21] Wakita T, Pietschmann T, Kato T, et al. Production of infectious hepatitis C virus in tissue culture from a cloned viral genome. Nat Med 2005;11:791–6.
[22] Blight KJ, Kolykhalov AA, Rice CM. Efficient initiation of HCV RNA replication in cell culture. Science 2000;290:1972–4.
[23] Frese M, Schwarzle V, Barth K, et al. Interferon-gamma inhibits replication of subgenomic and genomic hepatitis C virus RNAs. Hepatology 2002;35:694–703.
[24] Guo JT, Bichko VV, Seeger C. Effect of alpha interferon on the hepatitis C virus replicon. J Virol 2001;75:8516–23.
[25] Yokota T, Sakamoto N, Enomoto N, et al. Inhibition of intracellular hepatitis C virus replication by synthetic and vector-derived small interfering RNAs. EMBO Rep 2003;4:602–8.
[26] Tanabe Y, Sakamoto N, Enomoto N, et al. Synergistic inhibition of intracellular hepatitis C virus replication by combination of ribavirin and interferon- alpha. J Infect Dis 2004;189:1129–39 [Epub 2004 Mar 16].
[27] Kato T, Date T, Miyamoto M, et al. Efficient replication of the genotype 2a hepatitis C virus subgenomic replicon. Gastroenterology 2003;125:1808–17.
[28] Kanazawa N, Kurosaki M, Sakamoto N, et al. Regulation of hepatitis C virus replication by interferon regulatory factor-1. J Virol 2004;78:9713–20.
[29] Yanai Y, Sanou O, Kayano T, et al. Analysis of the antiviral activities of natural IFN-alpha preparations and their subtype compositions. J Interferon Cytokine Res 2001;21:835–41.
[30] Klein SB, Blatt LM, Taylor MW. Consensus interferon induces peak mRNA accumulation at lower concentrations than interferon-alpha 2a. J Interferon Res 1993;13:341–7.
[31] Nakagawa M, Sakamoto N, Enomoto N, et al. Specific inhibition of hepatitis C virus replication by cyclosporin A. Biochem Biophys Res Commun 2004;313:42–7.
[32] Kimball PM, Kerman RH, Kahan BD. Sensitivity of intracellular signals responsible for cell cycle progression to cyclosporine. Transplantation 1990;49:186–91.
[33] Colombani PM, Bright EC, Wells M, Hess AD. Drug-drug interaction between cyclosporine and agents affecting calcium-dependent lymphocyte proliferation. Transplant Proc 1989;21:840–1.
[34] Novick D, Cohen B, Rubinstein M. The human interferon alpha/beta receptor: characterization and molecular cloning. Cell 1994;77:391–400.
[35] Domanski P, Witte M, Kellum M, et al. Cloning and expression of a long form of the beta subunit of the interferon alpha beta receptor that is required for signaling. J Biol Chem 1995;270:21606–11.
[36] Lutfalla G, Holland SJ, Cinato E, et al. Mutant U5A cells are complemented by an interferon-alpha beta receptor subunit generated by alternative processing of a new member of a cytokine receptor gene cluster. EMBO J 1995;14:5100–8.
[37] Yamaoka T, Kojima S, Ichi S, Kashiwazaki Y, Koide T, Sokawa Y. Biologic and binding activities of IFN-alpha subtypes in ACHN human renal cell carcinoma cells and Daudi Burkitt's lymphoma cells. J Interferon Cytokine Res 1999;19:1343–9.
[38] Soh J, Mariano TM, Lim JK, et al. Expression of a functional human type I interferon receptor in hamster cells: application of functional yeast artificial chromosome (YAC) screening. J Biol Chem 1994;269:18102–10.
[39] Cleary CM, Donnelly RJ, Soh J, Mariano TM, Pestka S. Knockout and reconstitution of a functional human type I interferon receptor complex. J Biol Chem 1994;269:18747–9.
[40] Cook JR, Cleary CM, Mariano TM, Izotova L, Pestka S. Differential responsiveness of a splice variant of the human type I interferon receptor to interferons. J Biol Chem 1996;271:13448–53.
[41] Ozes ON, Reiter Z, Klein S, Blatt LM, Taylor MW. A comparison of interferon-Con1 with natural recombinant interferons-alpha: antiviral, antiproliferative, and natural killer-inducing activities. J Interferon Res 1992;12:55–9.
[42] Tong MJ, Reddy KR, Lee WM, et al. Treatment of chronic hepatitis C with consensus interferon: a multicenter, randomized, controlled trial. Consensus Interferon Study Group. Hepatology 1997;26:747–54.

J Gastroenterol 2004; 39:563–569
DOI 10.1007/s00535-003-1343-0

Journal of Gastroenterology

Methylation status of suppressor of cytokine signaling-1 gene in hepatocellular carcinoma

HIDEYUKI MIYOSHI[1], HAJIME FUJIE[1], KYOJI MORIYA[1], YOSHIZUMI SHINTANI[1], TAKEYA TSUTSUMI[1], MASATOSHI MAKUUCHI[2], SATOSHI KIMURA[1], and KAZUHIKO KOIKE[1]

[1] Department of Internal Medicine, Graduate School of Medicine, University of Tokyo, 7-3-1 Hongo, Bunkyo-ku, Tokyo 113-8655, Japan
[2] Department of Hepatobiliary and Pancreatic Surgery, Graduate School of Medicine, University of Tokyo, Tokyo, Japan

Editorial on page 598

Background. Silencing of the suppressor of cytokine signaling (*SOCS-1*) by aberrant methylation at the CpG island in the coding region gene has been reported in hepatocellular carcinoma (HCC). However, principally, it is methylation in the 5′-noncoding region but not that in the coding region which determines the regulation of gene expression. ***Methods.*** Methylation-specific PCR was performed for the analysis of methylation status both in the 5′-noncoding region and the CpG island of *SOCS-1* from 22 HCC tissue samples with adjacent non-HCC tissue samples and from two cell lines. ***Results.*** Using primers in the CpG island, 9 of 22 HCC samples exhibited aberrant methylation of *SOCS-1*, while only 1 of 22 adjacent non-HCC samples did so. The unmethylation pattern was detected in 1 of 22 HCC and in 5 of 22 non-HCC samples. Thus, aberrant methylation of SOCS-1 was significantly associated with HCC (P = 0.0076 by Fisher's exact test). Using primers in the 5′-noncoding region, aberrant methylation was observed in 12 of 22 HCC and in 2 non-HCC samples. The unmethylated pattern was observed in 5 of 22 HCC and in 10 of 22 non-HCC samples (P = 0.0042). There was no significant correlation between the methylation status of *SOCS-1* and clinicopathological findings, such as the presence or absence of cirrhosis or the histological grade of HCC. ***Conclusions.*** Aberrant methylation of the *SOCS-1* had a significant correlation with HCC. The rate of aberrant methylation was similar in the 5′-noncoding region and in the CpG island. Aberrant methylation of *SOCS-1* may be associated with hepatocarcinogenesis, although further studies are necessary.

Received: July 9, 2003 / Accepted: November 7, 2003
Reprint requests to: K. Koike

Key words: *SOCS-1*, hepatocellular carcinoma, methylation

Introduction

The majority of cases of hepatocellular carcinoma (HCC) are associated with hepatitis B or C viral infection.[1,2] Despite the absence of an appropriate in vitro replication system or a practical infectious animal model system, the mechanism underlying hepatocarcinogenesis in human hepatitis viral infection is on a stable path to elucidation, albeit slowly. Both the direct and indirect effects of hepatitis viruses on HCC development have been shown.[3–6] Accumulation of gene aberrations, such as inactivation of tumor suppressor genes or activation of oncogenes, which may be induced through inflammation-mediated continuous death of hepatocytes followed by regeneration, is considered to be one of the mechanisms underlying hepatocarcinogenesis.[3,4] On the other hand, viral gene products are suggested to contribute to HCC development by their direct effects on hepatocytes.[5–8] Such direct effects have been demonstrated by the use of model systems including mice.[5–7]

In contrast, gene alterations that play pivotal roles in hepatocarcinogenesis in the majority of HCC tissues have not been identified yet. To date, the genes for the APC-axin-GSK-3β complex may be only one of such candidate genes.[9,10] Such gene alterations include not only mutations in the genes per se but also epigenetic changes, which lead to either suppression or augmentation of gene expression. A change in the methylation state of the gene is one of the epigenetic changes that are associated with carcinogenesis. A possible role of methylation of genes in HCC development has been reported[11] for a tumor suppressor gene, $p16^{INK4}$: $p16^{INK4}$ expression was downregulated by methylation of the

control region. Expression of some other cancer-related genes may also be inhibited by methylation.

Silencing of the suppressor of cytokine signaling-1 (SOCS-1; also known as SSI-1 or JAB) is a member of the SOCS protein family. It switches off cytokine signaling by directly interacting with Janus kinase (JAK) proteins; its expression renders cells unresponsive to interleukin-6 stimulation.[12] The SH2 domain of SOCS-1 binds to a JH1 domain of JAK2 and inhibits its phosphorylation, downregulating the JAK/STAT pathway.[12,13] SOCS-1 inhibits the biological effects of cytokines in vivo; its forced expression interrupts macrophage differentiation induced by IL-6 and suppresses CD23 expression induced by IL-4.[12,13] Thus, SOCS-1 modulates the immune system through interacting with the cytokine network.

Recently, *SOCS-1*-deficient mice have been shown to die within 3 weeks after birth from a myeloproliferative disorder resulting from unbridled interferon (IFN)-γ and tumor necrosis factor (TNF)-α signaling.[14] As a negative regulator of cytokine signaling, *SOCS-1* is now a candidate gene for inactivating mutations that will favor the development of malignancies; SOCS-1 may inhibit cell proliferation induced by oncogenic forms of other known SOCS-1-interacting proteins. In addition to the results in hematopoietic neoplasia, recently suppression of SOCS-1 expression has been reported in HCC, in which the CpG-rich domain in the coding region of *SOCS-1* was found to be aberrantly methylated.[15] However, in general, it is the methylation of the 5′ non-coding region, which contains the promoter, but not that of the coding region, which determines gene expression.[16,17] We therefore conducted this experiment to evaluate the methylation status of the *SOCS-1* in HCC by methylation-specific PCR (MSPCR) using primers located both in the 5′-noncoding region and in the CpG-rich domain (CpG island) of the coding region.

Patients and methods

Patients

We studied 22 patients (19 males and 3 females; median age, 63.5 years) with HCC who had underlying chronic hepatitis C with or without cirrhosis (8 without and 14 with cirrhosis), all of whom underwent hepatectomy between 1997 and 2000 at the University of Tokyo Hospital. This study was approved by the ethics review committee of the institute, and carried out in accordance with the World Medical Association Helsinki Declaration, adopted in 1964 and amended in 1996. Informed consent was obtained from each patient. All the patients were positive for anti-hepatitis C virus (HCV) confirmed by the second-generation enzyme immunoassay and HCV-RNA by reverse-transcriptase-polymerase chain reaction (RT-PCR), and none were positive for serum hepatitis B surface antigen (HBsAg). The clinicopathological features of the patients are shown in Table 1.

Tissue samples and cell lines

The cancerous (HCC) and noncancerous (non-HCC) liver tissue samples obtained from these patients were fixed in 10% formalin for hematoxylin and eosin staining, or immediately frozen and stored at −80°C until further use. The histological staging of the noncancerous tissues was performed according to the European classification for chronic hepatitis,[18] and that of cancerous tissue was based on the TNM classification.[19] All the 22 tumors were classified as advanced HCCs: 5 well-, 14 moderately, and 3 poorly differentiated HCCs (see Table 1). Human HCC cell lines PLC/PRF/5, HuH-7, and the B-cell line, BJAB, were obtained from the American Type Culture Collections. The cells were grown in Dulbecco's modified Eagle's medium (DMEM) supplemented with 10% fetal bovine serum.

DNA preparation and bisulfite treatment

Genomic DNA was extracted from the frozen tissues by standard proteinase K digestion and phenol/chloroform extraction.[20] Then, bisulfite modification of genomic DNA was carried out as described previously[21] with slight modification. Briefly, DNA (1 μg) in a volume of 20 μl was denatured by NaOH at a final concentration at 0.3 M for 15 min at 37°C. Then, 113 μl 3.6 M sodium bisulfite (Sigma-Aldrich, St. Louis, MO, USA) at pH 5 and 7.2 μl 10 mM hydroquinone (Sigma-Aldrich), both freshly prepared, were added and mixed well. Then, the samples were incubated under mineral oil at 95°C for 15 min followed by incubation at 50°C for 4 h, and this cycle was repeated 15 times. Modified DNA was purified and resuspended in 50 μl water. The modification was completed by adding NaOH at a final concentration of 0.3 M for 5 min at room temperature, after which ethanol precipitation was carried out.

Genomic and methylation-specific PCR (MSPCR)

Bisulfite-modified and unmodified DNA was subjected to amplification using the PCR method. Primers used for the PCR in the current study are shown in Table 2. Amplification was carried out in a thermal cycler for a total of 35 cycles consisting of 95°C for 30 s, 60°C for 30 s, and 30 s at 72°C in 50 μl reaction mixture containing 200 mM deoxynucleoside triphosphates (dNTPs), 1.0 mM of each primer, and 1× PCR buffer [16.6 mM

Table 1. SOCS-1 gene methylation and clinicopathological findings of 22 hepatocellular carcinoma (HCC) patients

		Methylation of SOCS-1							
		CpG island				5′-noncoding			
		M[a]		U[a]		M[a]		U[a]	
	n	HCC	nHCC	HCC	nHCC	HCC	nHCC	HCC	nHCC
Sex									
Male	19	7	1	1	4	10	2	5	9
Female	3	2	0	0	1	2	0	0	1
Cirrhosis									
−	8	2	0	0	1	3	0	2	4
+	14	7	1	1	4	9	3	3	5
Pathology of HCC[b]									
WD	5	3	0	0	2	3	0	1	3
MD	14	4	1	1	2	7	1	3	6
PD	3	2	0	0	1	2	1	1	0
Tumor size (cm)									
<2	5	2	0	0	0	2	2	2	1
≥2	17	7	1	1	5	10	0	3	9
Vascular invasion									
Absent	19	8	1	1	4	11	2	5	9
Present	3	1	0	0	1	1	0	0	1
Distant metastasis[c]									
M0	20	9	1	1	4	12	1	4	10
M1	2	0	0	0	1	0	1	1	0
Stage grouping[c]									
I	4	1	0	0	0	1	2	2	1
II	5	3	0	0	2	3	0	1	2
III	11	4	1	0	3	6	1	2	7
IV	2	1	0	1	0	2	0	0	0
Overall	22	9* (41%)	1* (5%)	1* (5%)	5* (23%)	12* (55%)	2* (9%)	5* (23%)	10* (46%)

[a] M, hypermethylated pattern; U, unmethylated pattern; not all samples were informative for methylation status
[b] WD, well-differentiated; MD, moderately differentiated; PD, poorly differentiated
[c] According to TNM classification
* $P < 0.01$ when the association of HCC and methylation was judged by Fisher's exact test for each of CpG island and 5′-noncoding region

Table 2. Polymerase chain reaction (PCR) primers used in the current study

	Sequence	Position
Forward		
HM1F	TTCGCGTGTATTTTTAGGTCGGTC	(400–423)
HM2F	GAGTATTCGCGTGTATTTTTAGG	(395–417)
UM1F	TTATGAGTATTTGTGTGTATTTTTAGGTTGGTT	(391–423)
UM2F	TGAGTATTTGTGTGTATTTTTAGG	(394–417)
UMPF-M	GTTCGGTTTCGTTTAGTTTTCGAGG	(−708–684)
UMPF-U	GTTTGGTTTTGTTTAGTTTTTGAGG	(−708–684)
Reverse		
HM1R	CGACACAACTCCTACAACGACCG	(537–559)
UM1R	CACTAACAACACAACTGGTACAACAACCA	(537–565)
UM2R	CAACACAACTCCTACAACAACCA	(543–565)
UMPR-M	ACCCCGACCGACCGCGATCTC	(−590–570)
UMPR-U	ACCCCAACCAACCACAATCTC	(−590–570)

ammonium sulfate, 67 mM Tris-HCl (pH 8.8), 6.7 mM $MgCl_2$, 10 mM 2-mercaptoethanol, and 0.001% (w/v) gelatin] and 1.25 units of Ampli-Taq polymerase (Perkin-Elmer Cetus, Norwalk, CT, USA). The PCR products were separated in a 2.0% agarose gel and visualized by staining with ethidium bromide.

Reverse transcription (RT)-PCR

Total RNA was extracted from cells using RNAzolB (TEL-TEST, Friendswood, TX, USA). Three micrograms of total RNA were reverse transcribed by Superscript II (Gibco-BRL, Gaithersburg, MD, USA) using oligo(dT) primer and subjected to PCR. Primers for RT-PCR of SOCS-1 gene expression were as follows: forward, 5′-CACGCACTTCCGCACATTCC-3′; reverse, 5′-TCCAGCAGCTCGAAGAGGCA-3′. For the RT-PCR, the quantity of cDNA template and the number of amplification cycles were optimized to ensure that the reaction was terminated during the linear phase of product amplification, so that semiquantitative comparisons of the mRNA abundance between different samples were possible. RT-PCR with glyceraldehyde phosphate dihydrogenase (GAPDH) primers was done to adjust the amounts of RNA in each experiment.

Statistical analysis

Fisher's exact test was used for statistical evaluation, and P values below 0.05 were considered significant.

Results

Methylation status of SOCS-1 in cultured cell lines

First, the methylation status of the CpG island in the coding region of *SOCS-1* was analyzed in cell lines by MSPCR using the primer sets, HM1F+HM1R and UM1F+UM1R, according to the method of Yoshikawa et al.[15] MSPCR using these primers, however, could not determine the methylation status of the gene: the use of the primers resulted in dimer formation without methylation- or unmethylation-specific bands. We therefore redesigned new sets of primers located in the CpG island of *SOCS-1* (Table 2; HM2F+HM1R for detecting a methylation-specific band and UM2F+UM2R for an unmethylation-specific band). MSPCR with these sets of primers enabled successful detection of methylation- and unmethylation-specific bands in PLC/PRF/5 cells (Fig. 1). The unmethylation-specific band alone was detected in HuH-7 cells, in agreement with the previous report.[15]

Analysis using the primers located in the 5′-noncoding region (see Table 2) yielded a similar pattern, excluding that there were both methylation- and unmethylation-specific bands also in HuH-7 cells (Fig. 1). Accordingly, the primer sets HM2F+HM1R and UM2F+UM2R were used for the analysis of the methylation status of the CpG island, and UMPF-M+UMPR-M and UMPF-U+UMPR-U were used for the 5′-noncoding region, thereafter.

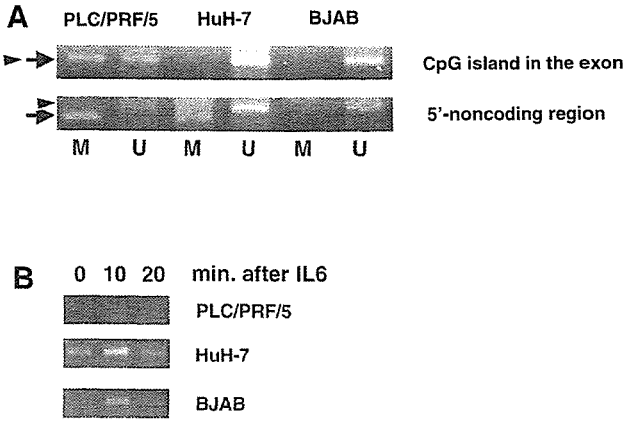

Fig. 1. Genomic and methylation-specific (MSPCR) analysis of cultured hepatoma cell lines in the CpG island and 5′-no-coding region of the *SOCS-1* gene. DNA from human hepatoma cell lines, PLC/PRF/5 and HuH-7, and a B-cell line, BJAB, was analyzed by MSPCR after bisulfite treatment as described in the Patients and methods section. **A** MSPCR with the primers in the CpG island and those in the 5′-noncoding region. **B** RT-PCR showing the expression of SOCS-1 in cell lines before and after the addition of IL-6 (10 ng/ml). The *arrow* indicates the position of the methylation-specific band; the *arrowhead* indicates the position of the unmethylation-specific band. *M*, MSPCR with methylation-specific primers; *U*, MSPCR with unmethylation-specific primers

Expression of SOCS-1 mRNA in cell lines

The expression of SOCS-1 was determined by semiquantitative RT-PCR. Although SOCS-1 expression was abundant in HuH-7 and BJAB cells in the baseline and was enhanced by the addition of IL-6 (10 ng/ml), only marginal expression and no enhancement were detected in PLC/PRF/5 cells. These results are consistent with the methylation status that was determined in the current study and with the expression status in the baseline that was observed in a previous report.[15]

Methylation status of SOCS-1 in human tumor samples

Then, DNA extracted from human HCC and non-HCC tissues was tested for the methylation status of the *SOCS-1* by MSPCR. Only 10 and 6 tissue samples were informative for determining a methylation-specific band

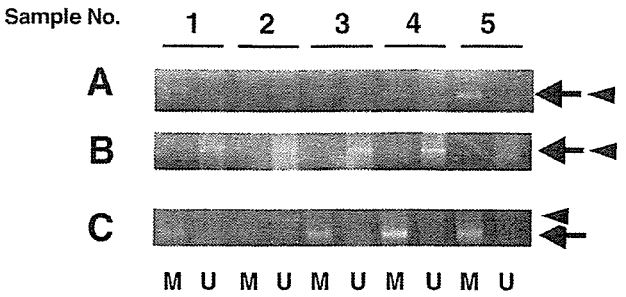

Fig. 2. MSPCR analysis of the CpG island and 5′-noncoding region of the *SOCS-1* from 22 HCC tissue samples. With the same primers used in Fig. 1, 22 pairs of HCC and non-HCC samples were analyzed by MSPCR. Representative cases are shown. Samples *1* and *2* were well-differentiated HCC, *3* and *4* were moderately differentiated HCC, and *5* was poorly differentiated HCC. Panel **B** shows their non-HCC counterparts. **A** MSPCR of DNA from HCC tissue samples with the primers in CpG island. **B** MSPCR of DNA from non-HCC tissue samples with the primers in CpG island. **C** MSPCR of DNA from HCC tissue samples with the primers in 5′-noncoding region. The *arrow* indicates the position of the methylation-specific band; the *arrowhead* indicates the position of the unmethylation-specific band HCC, hepatocellular carcinoma; M, MSPCR with methylation-specific primers; U, MSPCR with unmethylation-specific primers

and an unmethylation-specific band, respectively, when the primers in the CpG island were used. In 9 HCC tissue samples the band indicative of aberrant methylation in the CpG island was detected, while the band indicating unmethylation was detected in 1 HCC tissue sample (Fig. 2). In contrast, in the corresponding non-HCC tissue samples, only 1 exhibited the methylation pattern, whereas the unmethylation pattern was observed in 5 non-HCC tissue samples. Thus, aberrant methylation of *SOCS-1* was significantly associated with HCC rather than with non-HCC tissues ($P = 0.0076$ by Fisher's exact test).

Using primers in the 5′-noncoding promoter region, 14 and 15 HCC tissue samples were informative for a methylation-specific band and an unmethylation-specific band, respectively. Aberrant methylation was observed in 12 HCC tissue samples whereas the unmethylation pattern was detected in 5 HCC tissue samples. In contrast, only 2 non-HCC tissues exhibited aberrant methylation whereas the unmethylation pattern was detected in 10 non-HCC tissues: there was also a significant correlation between HCC and aberrant methylation of *SOCS-1* ($P = 0.0042$).

Neither a methylation-specific nor an unmethylation-specific band in 12 HCC and 16 non-HCC tissues was detected using the primers in the CpG island and in 5 HCC and 10 non-HCC tissue samples using the primers in the 5′-noncoding promoter region, suggesting that *SOCS-1* in these tissues was in a mosaic state of methylation. This suggestion was examined using a hepatoma cell line HLF: neither a methylation- nor an unmethylation-specific band was detected, but after 5-azacytidine treatment of the cell line for 3 days, which cancels methylation of the gene,[22] an unmethylation-specific band appeared, demonstrating that *SOCS-1* in the cell line is methylated in a mosaic fashion. Consequently, *SOCS-1* gene expression was turned on as determined by RT-PCR.

Correlation between SOCS-1 methylation and clinicopathological findings

The relationship between the methylation status of *SOCS-1* and clinicopathological findings is shown in Table 1. When the methylation status in HCC tissue samples was correlated with parameters such as the presence or absence of cirrhosis as the underlying liver disease, the histological degree of HCC, tumor sizes, vascular invasion, distant metastasis, or tumor stages, no significant association was noted.

Discussion

In the current study, we analyzed the methylation status of *SOCS-1*, a negative regulator of the JAK/STAT pathway, by the MSPCR method. Using the primers located in the CpG island in the coding region, aberrant methylation was observed in 9 of 22 (41%) HCC tissue samples, and 12 of 22 (54.5%) HCC tissue samples by the use of primers in the 5′-noncoding region. The former rate is almost compatible with the incidence in a previous report.[14] It is notable that a similar or higher rate of aberrant methylation was detected in the 5′-noncoding promoter region of *SOCS-1*. It is established that methylation in the promoter region is essential in the regulation of (silencing) the genes.[16,17] The frequent occurrence of aberrant methylation in the promoter region of *SOCS-1* further supports the notion that the downregulation of SOCS-1 expression is common in human HCC. Very recently, methylation in the promoter of SOCS-1 gene was reported in pancreatic tumors.[23]

In our MSPCR analysis, a substantial number of samples showed neither the methylated nor unmethylated pattern. The reason for this dual negativity is unclear. One possibility is a mosaic methylation pattern that may exist in the *SOCS-1*. If not all the susceptible cytosine residues are methylation, i.e., a gene is methylated in a mosaic fashion, one cannot determine the methylation status by MSPCR. This possibility was confirmed using a hepatoma cell line, as shown in the Results section. Neither a methylation- nor an unmethylation-specific band was detected, but after

5-azacytidine treatment of the cell line for 3 days, which cancels methylation of the gene,[22] an unmethylation-specific band appeared, demonstrating that *SOCS-1* in the cell line is methylated in a mosaic fashion.

SOCS-1 transcription is activated by signal transducer and activator of transcription (STAT) and the resultant proteins negatively regulate the JAK/STAT pathways either by directly inhibiting JAKs or by binding to receptors and blocking further association with STATs. Of the eight SOCS family members, SOCS-1 is a negative regulator of IL-6 signals. The silencing of *SOCS-1* results in constitutive activation of the JAK/STAT pathway. Without negative feedback by SOCS-1, the downstream pathways and target genes are strongly activated.[24] There are several lines of evidence supporting the idea that the JAK/STAT pathway may be involved in oncogenesis. The constitutive activation of the JAK/STAT pathway including STAT3 is observed in a number of transformed cells.[25] Thus, SOCS-1 is considered to be a tumor suppressor candidate, which chiefly has a role in the development of hematopoietic malignancies.[26] Also, an association of the SOCS-1 in hepatocarcinogenesis has recently been suggested.[15] There are a variety of gene products in the downstream of the JAK/STAT pathway, including c-*myc* or c-*fos*.[27] The activation of the pathway thus may cause an activation of oncogenes or growth-associated genes and eventually lead to oncogenesis. The precise role of SOCS-1 in hepatocarcinogenesis is currently unclarified and requires further study, but it might play an essential role in the majority of HCCs.

Our current results confirmed those of a previous study[14] and added a new piece of information on methylation of the promoter region of *SOCS-1*. However, the presence of cases negative for both methylation and unmethylation may limit the application of this technique for the analysis of hepatocarcinogenesis. In addition, recently the association between the core protein of hepatitis C virus and the JAK/STAT pathway has been reported as a potential proliferator of hepatocytes.[28] Besides aberrant methylation, association of SOCS-1 with HCV may cause a down-regulation of *SOCS-1* expression. In relation to this issue, it is interesting to note that a few patients in our series exhibited aberrant methylation of *SOCS-1* in the adjacent non-HCC tissue samples. Infection with HCV, which is present in all patients, may be associated with *SOCS-1* expression in human HCC tissues. Further studies are necessary for deciphering the complicated involvement of the SOCS-1 and JAK/STAT pathway in hepatocarcinogenesis, possibly in association with HCV infection.

References

1. Chen CJ, Yu MW, Liaw YF. Epidemiological characteristics and risk factors of hepatocellular carcinoma. J Gastroenterol Hepatol 1997;12:S294–308.
2. Saito I, Miyamura T, Ohbayashi A, Harada H, Katayama T, Kikuchi S, et al. Hepatitis C virus infection is associated with the development of hepatocellular carcinoma. Proc Natl Acad Sci U S A 1990;87:6547–9.
3. Robinson WS. Molecular events in the pathogenesis of hepadnavirus-associated hepatocellular carcinoma. Annu Rev Med 1994;45:297–323.
4. Umeda T, Hino O. Molecular aspects of human hepatocarcinogenesis mediated by inflammation: from hypercarcinogenic state to normo- or hypocarcinogenic state. Oncology 2002;62:38–42.
5. Kim CM, Koike K, Saito I, Miyamura T, Jay G. HBx gene of hepatitis B virus induces liver cancer in transgenic mice. Nature (Lond) 1991;351:317–20.
6. Moriya K, Fujie H, Shintani Y, Yotsuyanagi H, Tsutsumi T, Matsuura Y, et al. The core protein of hepatitis C virus induces hepatocellular carcinoma in transgenic mice. Nat Med 1998; 41065–7.
7. Lerat H, Honda M, Beard MR, Loesch K, Sun J, Yang Y, et al. Steatosis and liver cancer in transgenic mice expressing the structural and nonstructural proteins of hepatitis C virus. Gastroenterology 2002;122:352–65.
8. Koike K, Tsutsumi T, Fujie H, Shintani Y, Moriya K. Role of hepatitis viruses in hepatocarcinogenesis. Oncology 2002;62:29–37.
9. Satoh S, Daigo Y, Furukawa Y, Kato T, Miwa N, Nishiwaki T, et al. AXIN1 mutations in hepatocellular carcinomas, and growth suppression in cancer cells by virus-mediated transfer of AXIN1. Nat Genet 2000;24:245–50.
10. Fujie H, Moriya K, Shintani Y, Tsutsumi T, Takayama T, Makuuchi M, et al. Frequent β-catenin aberration in human hepatocellular carcinoma. Hepatol Res 2001;20:39–51.
11. Matsuda Y, Ichida T, Matsuzawa J, Sugimura K, Asakura H. p16(INK4) is inactivated by extensive CpG methylation in human hepatocellular carcinoma. Gastroenterology 1999;116:394–400.
12. Starr R, Willson TA, Viney EM, Murray LJ, Rayner JR, Jenkins BJ, et al. A family of cytokine-inducible inhibitors of signaling. Nature (Lond) 1997;387:917–21.
13. Endo TA, Masuhara M, Yokouchi M, Suzuki R, Sakamoto H, Mitsui K, et al. A new protein containing an SH2 domain that inhibits JAK kinases. Nature 1997;387:921–4.
14. Naka T, Matsumoto T, Narazaki M, Fujimoto M, Morita Y, Ohsawa Y, et al. Accelerated apoptosis of lymphocytes by augmented induction of Bax in SSI-1 (STAT-induced STAT inhibitor-1) deficient mice. Proc Natl Acad Sci U S A 1998;95: 15577–82.
15. Yoshikawa H, Matsubara K, Qian GS, Jackson P, Groopman JD, Manning JE, et al. SOCS-1, a negative regulator of the JAK/STAT pathway, is silenced by methylation in human hepatocellular carcinoma and shows growth-suppression activity. Nat Genet 2001;28:29–35.
16. Jaenisch R, Bird A. Epigenetic regulation of gene expression: how the genome integrates intrinsic and environmental signals. Nat Genet 2003;33:245–54.
17. Herman JG, Baylin SB. Promoter-region hypermethylation and gene silencing in human cancer. Curr Top Microbiol Immunol 2000;249:35–54.
18. Desmet VJ, Gerber M, Hoofnagle JH, Manns M, Scheuer PJ. Classification of chronic hepatitis: diagnosis, grading and staging. Hepatology 1994;19:1513–20.
19. Hermanek P, Sobin LH. UICC TNM classification of malignant tumors. 4th ed. Berlin: Splinger; 1987.
20. Yotsuyanagi H, Yasuda K, Iino S, Moriya K, Fujie H, Shintani Y, et al. Persistent viremia after recovery from self-limited acute hepatitis B. Hepatology 1998;27:1377–82.

21. Herman JG, Graff JR, Myohanen S, Nelkin BD, Baylin SB. Methylation-specific PCR: a novel PCR assay for methylation status of CpG islands. Proc Natl Acad Sci U S A 1996;93:9821–6.
22. Velicescu M, Weisenberger DJ, Gonzales FA, Tsai YC, Nguyen CT, Jones PA. Cell division is required for de novo methylation of CpG islands in bladder cancer cells. Cancer Res 2002;62:2378–84.
23. House MG, Guo M, Iacobuzio-Donahue C, Herman JG. Molecular progression of promoter methylation in intraductal papillary mucinous neoplasms (IPMN) of the pancreas. Carcinogenesis (Oxf) 2003;24:193–8.
24. Greenhalgh CJ, Miller ME, Hilton DJ, Lund PK. Suppressors of cytokine signaling: relevance to gastrointestinal function and disease. Gastroenterology 2002;123:2064–81.
25. Kishimoto T, Kikutani H. Knocking the SOCS off a tumor suppressor. Nat Genet 2001;28:4–5.
26. Rottapel R, Ilangumaran S, Neale C, La Rose J, Ho JM, Nguyen MH, et al. The tumor suppressor activity of SOCS-1. Oncogene 2002;21:4351–62.
27. Darnell JE Jr, Kerr IM, Stark GR. Jak-STAT pathways and transcriptional activation in response to IFNs and other extracellular signaling proteins. Science 1994;264:1415–21.
28. Yoshida T, Hanada T, Tokuhisa T, Kosai K, Sata M, Kohara M, et al. Activation of STAT3 by the hepatitis C virus core protein leads to cellular transformation. J Exp Med 2002;196:641–53.

GASTROENTEROLOGY 2004;126:840–848

BASIC–LIVER, PANCREAS, AND BILIARY TRACT

Hepatitis C Virus Infection and Diabetes: Direct Involvement of the Virus in the Development of Insulin Resistance

YOSHIZUMI SHINTANI,* HAJIME FUJIE,* HIDEYUKI MIYOSHI,* TAKEYA TSUTSUMI,* KAZUHISA TSUKAMOTO,† SATOSHI KIMURA,* KYOJI MORIYA,* and KAZUHIKO KOIKE*
Departments of *Internal Medicine and †Metabolic Diseases, Graduate School of Medicine, University of Tokyo, Tokyo, Japan

See editorial on page 917.

Background & Aims: Epidemiological studies have suggested a linkage between type 2 diabetes and chronic hepatitis C virus (HCV) infection. However, the presence of additional factors such as obesity, aging, or cirrhosis prevents the establishment of a definite relationship between these 2 conditions. *Methods:* A mouse model transgenic for the HCV core gene was used. *Results:* In the glucose tolerance test, plasma glucose levels were higher at all time points including in the fasting state in the core gene transgenic mice than in control mice, although the difference was not statistically significant. In contrast, the transgenic mice exhibited a marked insulin resistance as revealed by the insulin tolerance test, as well as significantly higher basal serum insulin levels. Feeding with a high-fat diet led to the development of overt diabetes in the transgenic mice but not in control mice. A high level of tumor necrosis factor-α, which has been also observed in human chronic hepatitis C patients, was considered to be one of the bases of insulin resistance in the transgenic mice, which acts by disturbing tyrosine phosphorylation of insulin receptor substrate-1. Moreover, administration of an anti-tumor necrosis factor-α antibody restored insulin sensitivity. *Conclusions:* The ability of insulin to lower the plasma glucose level in the HCV transgenic mice was impaired, as observed in chronic hepatitis C patients. These results provide a direct experimental evidence for the contribution of HCV in the development of insulin resistance in human HCV infection, which finally leads to the development of type 2 diabetes.

Approximately 200 million people are chronically infected with hepatitis C virus (HCV) in the world. Chronic HCV infection may lead to cirrhosis and hepatocellular carcinoma, thereby being a worldwide problem both in medical and socioeconomical aspects.[1,2] In addition, chronic HCV infection is a multifaceted disease, which is associated with numerous clinical manifestations, such as essential mixed cryoglobulinemia, porphyria cutanea tarda, and membranoproliferative glomerulonephritis.[3] Recent epidemiological studies have added another clinical condition, type 2 diabetes, to a spectrum of HCV-associated diseases.[4–7] However, the establishment of a definite causative relationship between HCV infection and diabetes is hampered by the presence of other factors such as obesity, aging, or liver injury in patients with chronic HCV infection.

Type 2 diabetes is a complex, multisystem disease with a pathophysiology that includes a defect in insulin secretion, increased hepatic glucose production, and resistance to the action of insulin, all of which contribute to the development of overt hyperglycemia.[8,9] Although the precise mechanisms whereby these factors interact to produce glucose intolerance and diabetes are uncertain, it has been suggested that the final common pathway responsible for the development of type 2 diabetes is the failure of the pancreatic β-cells to compensate for the insulin resistance. Hyperinsulinemia in the fasting state is observed relatively early in type 2 diabetes, but it is considered to be a secondary response that compensates for the insulin resistance.[8,9] Overt diabetes occurs over time when pancreatic β-cells bearing the burden of increased insulin secretion fail to compensate for the insulin resistance.

In this study, to elucidate the role of HCV in a possible association between diabetes and HCV infection, transgenic mice that carry the core gene of HCV[10,11] were analyzed. We found that these mice developed insulin resistance. An addition of a high-calorie diet led to the development of type 2 diabetes by dis-

Abbreviations used in this paper: EDL, extensor digitorum longus; ELISA, enzyme-linked immunosorbent assay; FPG, fasting plasma glucose; HCV, hepatitis C virus; IRS, insulin receptor substrate; JNK, c-Jun N-terminal kinase; TNF-α, tumor necrosis factor-α.

0016-5085/04/$30.00
doi:10.1053/j.gastro.2003.11.056

rupting the balance between insulin resistance and secretion.

Materials and Methods

Transgenic Mice

The production of HCV core gene transgenic mice has been described previously.[11] Briefly, the core gene from HCV of genotype 1b, which is placed downstream of a transcriptional regulatory region from the hepatitis B virus, was introduced into C57BL/6 mouse embryos (Clea Japan, Tokyo, Japan). The mice were cared for according to institutional guidelines, fed an ordinary chow diet (Funabashi Farms, Funabashi, Japan), and maintained in a specific pathogen-free state. At an indicated time, the mice were fed a high-fat diet (Oriental Yeast Co., Ltd., Tokyo, Japan) for up to 2 months. Caloric content of food was 4.70 kcal/g for high-fat diet and 3.56 kcal/g for ordinary diet. The high-fat diet contains 18.5% protein, 22.1% fat (4.7% vegetable fat and 17.4% animal fat), 5.4% ash, 2.5% fiber, 6.5% moisture, and 45.0% carbohydrate, and the ordinary diet contains 22.4% protein, 5.7% fat, 6.6% ash, 3.1% fiber, 7.7% moisture, and 54.5% carbohydrate. Because there is a sex preference in the development of liver lesion in the transgenic mice, we used only male mice that were heterozygously transgenic for the core gene, and as controls we used nontransgenic litter mates of the transgenic mice. Transgenic mice carrying the HCV envelope genes under the same regulatory region as that in the core gene transgenic mice were also used as controls.[12] At least 5 mice were used in each experiment and the data were subjected to statistical analysis.

Glucose Tolerance Test

The mice were fasted for >16 hours before the study. D-Glucose (1g/kg body weight) was administered by intraperitoneally (IP) injection to conscious mice. Blood was drawn at different time points from the orbital sinus, and plasma glucose concentrations were measured by using an automatic biochemical analyzer DRI-CHEM 3000V (Fuji Film, Tokyo, Japan). The levels of serum insulin were determined by radioimmunoassay (BIOTRAK; Amersham Pharmacia Biotech, Piscataway, NJ) with rat insulin as a standard.

Insulin Tolerance Test

The mice were fed freely and then fasted during the study period. Human insulin (1 U/kg body weight) (Humulin; Novo Nordisk, Denmark) was administered by IP injection to fasted conscious mice, and glucose concentrations were determined at the time points indicated. Values were normalized to the baseline glucose concentration at the administration of insulin.

Morphometric Analysis

Sections of the pancreas were prepared and evaluated for morphometry after H&E staining or immunostaining. Relative islet area and islet number were determined with an image analyzer (QUE-2; Olympus Optical Co., Tokyo, Japan).

Enzyme-Linked Immunosorbent Assay

ELISA for mouse tumor necrosis factor (TNF)-α was performed using a commercially available mouse TNF-α ELISA kit (BioSource International, Camarillo, CA). Samples were prepared as reported previously.[13] Briefly, the liver of transgenic and control mice were lysed with a buffer containing 1% Tween 80, 10 mmol/L Tris-HCl [pH 7.4], 1 mmol/L EDTA, 0.05% sodium azide, 2 mmol/L PMSF, and the Protease Inhibitor Cocktail (Complete; Roche Molecular Biochemicals, Indianapolis, IN) and homogenized on ice for 20 seconds. The homogenates were centrifuged at 11,000 × *g* for 10 minutes at 4° C, and the supernatants were collected and assayed. ELISA was performed in triplicate for each sample. The concentrations of the cytokines in the liver were normalized by determining the amount of total protein in each sample using the BCA Protein Assay Kit (Pierce, Rockford, IL).

Immunoprecipitation and Western Blotting

For immunoprecipitation studies, liver tissues were homogenized in lysis buffer (10 mmol/L Tris-HCl at pH 7.5, 150 mmol/L NaCl, 10 mmol/L sodium pyrophosphate, 1.0 mmol/L β-glycerophosphate, 1.0 mmol/L sodium orthovanadate [Na_3VO_4], 50 mmol/L sodium fluoride [NaF], the Protease Inhibitor Cocktail [Complete, Roche Molecular Biochemicals], and 1.0% Triton X-100), and homogenates were precipitated with an anti–insulin receptor substrate (IRS)-1 or anti–IRS-2 rabbit polyclonal antibody (UBI, Lake Placid, NY) and then with Sepharose 4B beads (Amersham Biosciences). Resulting pellets were washed 3 times and then subjected to Western blotting. Pellets were resuspended in Western sample buffer (5% β-mercaptoethanol, 2% sodium dodecyl sulfate, 62.5 mmol/L Tris-HCl, 1 mmol/L EDTA, 10% glycerol), and then subjected to 2%–15% gradient sodium dodecyl sulfate/PAGE (PAG Mini "DAIICHI" 2/15 (13W), Daiichi Diagnostics, Tokyo, Japan), and electrotransferred to polyvinylidene difluoride membranes (Immobilon-P, Millipore, Bedford, MA). The filter was then reacted with antiphosphorylated tyrosine (Santa Cruz Biotechnology Inc., Santa Cruz, CA), antiphosphorylated serine (Cell Signaling Technology, Inc., Beverly, MA), anti–IRS-1 or anti–IRS-2 mouse monoclonal antibody (BD Biosciences, Lexington, KY), followed by immunostaining with secondary biotinylated IgG (Vector Labs, Inc., Burlingame, CA) and visualization using an ECL kit (Amersham Intl., Buckinghamshire, UK).[14]

Hyperinsulinemic-Euglycemic Clamp

Mice underwent a hyperinsulinemic-euglycemic clamp using D-[3-^{3}H]glucose (NEN Life Science, Boston, MA) to measure the rate of glucose appearance and hepatic glucose production (HGP) as described previously.[15] Three days after jugular catheter placement, a hyperinsulinemic-euglycemic clamp was conducted with a continuous infusion of human

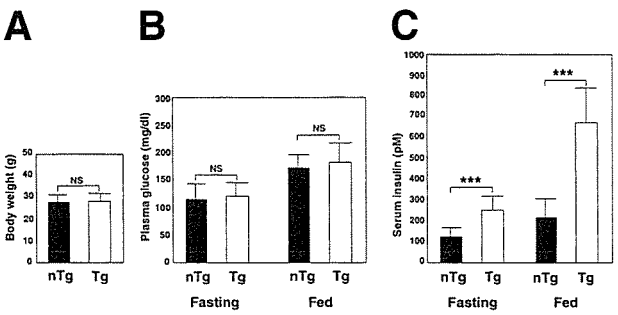

Figure 1. Altered glucose homeostasis in hepatitis C virus core gene transgenic mice. (*A*) Body weight of 2-month-old mice (n = 10 in each group). (*B*) Plasma glucose levels in fasting or fed mice (n = 10 in each group). (*C*) Serum insulin levels in fasting or fed mice (n = 10 in each group). The insulin level was significantly higher in the core gene transgenic mice than in control mice. Values are mean ± standard error; $***P < 0.001$; NS, statistically not significant; nTg, nontransgenic mice; Tg, transgenic mice.

insulin to raise serum insulin within a physiological range. Blood samples were drawn at intervals for the immediate measurement of blood glucose concentration, and 20% glucose was infused at variable rates to maintain blood glucose at ca. 125 mg/dL. All infusions were done using microdialysis pumps (KD Scientific Inc., Boston, MA). The rate of glucose appearance (mg/kg per minute), which equals the rate of total body glucose utilization during steady state, was calculated as the ratio of the rate of infusion of [3-^{3}H]glucose and the steady state plasma [^{3}H-]glucose specific activity. HGP (mg/kg/min) during clamps was determined by subtracting the glucose infusion rate from the rate of glucose appearance.

Glucose Uptake by Skeletal Muscle

The extensor digitorum longus (EDL) or soleus muscle was excised from 2-month-old mice and exposed to insulin at the indicated concentrations. 2-Deoxyglucose uptake was determined as described previously.[16]

Treatment With Anti-TNF-α Antibody

To suppress TNF-α, a dose of 200 μg/mouse of neutralizing hamster monoclonal antibody (TN3-19.12, Santa Cruz Biotechnology Inc.) was administered by IP injection on days 1 and 4, and plasma glucose and insulin levels were determined at day 5.[17]

Statistical Analysis

The results are expressed as means ± standard error. The significance of the difference in means was determined by Student *t* test or Mann–Whitney *U* test whenever appropriate. $P < 0.05$ was considered significant.

Results

Hyperinsulinemia and Insulin Resistance in Transgenic Mice

At the age between 1 and 12 months, there was no significant difference in body weight between the core gene transgenic mice and control mice. Figure 1*A* shows body weight of 2-month-old mice. Fasting plasma glucose (FPG) levels were slightly elevated in the core gene transgenic mice compared with control mice, but the difference was not significant ($P = 0.79$, Figure 1*B*). In contrast, there was a marked increase in the level of serum insulin in the core gene transgenic mice than control mice ($P < 0.001$, Figure 1*C*). Hyperinsulinemia was observed in the core gene transgenic mice as early as 1 month old. These findings suggest that decreased responsiveness to the hormone may have resulted in compensatory hyperinsulinemia. Administration of glucose to 2-month-old core gene transgenic mice revealed mild glucose intolerance compared with control mice of the same age, but the difference was not statistically significant at any time points measured (Figure 2*A*). HCV envelope gene transgenic mice of the same age, in which the envelope genes were expressed under the same transcriptional regulatory region as the core gene transgenic mice, did not manifest hyperinsulinemia or elevated FPG levels, indicating that not the transcriptional regulatory region used but the expressed gene itself is essential in this phenotype.

The insulin tolerance test conducted at the age of 2 months revealed that the reduction in plasma glucose concentration after IP insulin injection was impaired in the core gene transgenic mice, displaying higher plasma glucose levels than those in control mice at all time points measured (Figure 2*B*). At 40 and 60 minutes, the difference was statistically significant between transgenic

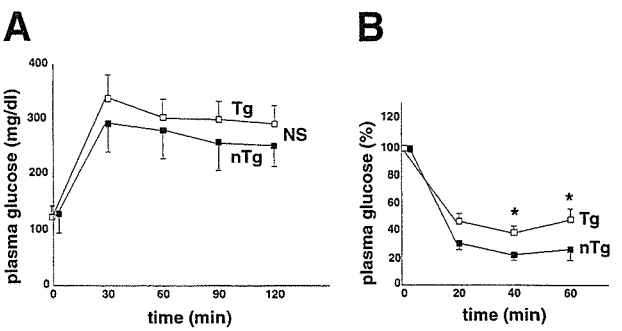

Figure 2. Insulin resistance in the core gene transgenic mice. (*A*) Glucose tolerance test (n = 5 in each group). Animals were fasted overnight (>16 hours). D-Glucose (1 g/kg body weight) was administered by IP injection to conscious mice, and plasma glucose levels were determined at the time points indicated. (*B*) Insulin tolerance test (n = 5 in each group). Human insulin (1 U/kg body weight) was administered by IP injection to fasted conscious mice and glucose concentrations were determined. Values were normalized to the baseline glucose concentration at the time of insulin administration. Values are mean ± standard error; $*P < 0.05$; NS, statistically not significant; nTg, nontransgenic mice; Tg, transgenic mice.

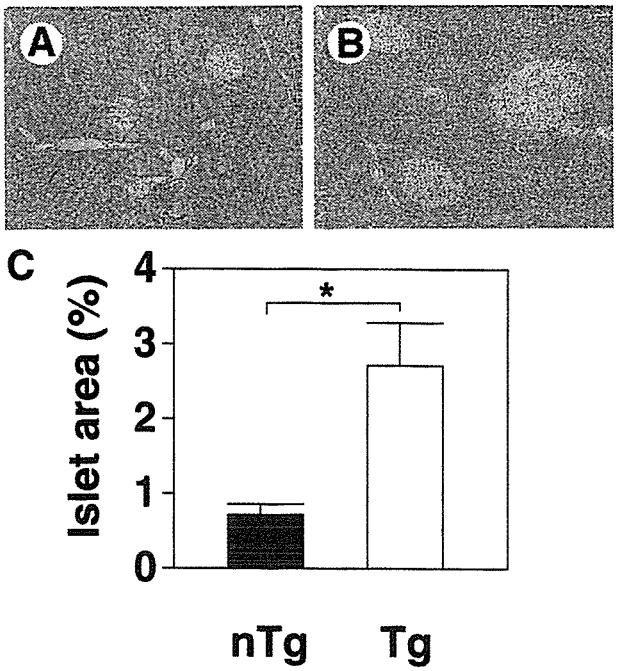

Figure 3. Analysis of pancreatic islet mass in the core gene transgenic and control mice. (*A* and *B*) Morphology of representative islets (H&E staining) from normal control mice (*A*) or the core gene transgenic mice (*B*). (*C*) Relative islet area, expressed as a percentage of the total stained pancreatic section, for control mice (nTg) and the core gene transgenic mice (Tg) (n = 10 in each group). Values are mean ± standard error; $*P < 0.05$.

and control mice (39.6 ± 1.3 vs. 24.4 ± 1.1 and 43.7 ± 2.1 vs. 26.4 ± 2.3, $P < 0.05$). These data are consistent with a defect in the actions of insulin on glucose disposal and/or production in the core gene transgenic mice.

Morphology of Pancreatic Islet Cells

Because a critical factor contributing to whether insulin resistance progresses to diabetes is the capacity of the pancreatic β-cells to respond to increased demands for insulin secretion, we evaluated the morphology of pancreatic islet cells by histologic examination. In the pancreas of HCV core gene transgenic mice, an approximately 3-fold increase in islet mass was observed (Figure 3, $P < 0.05$), which is consistent with β-cell compensation to insulin resistance. There was no infiltration of inflammatory cells within or surrounding the islets.

Feeding Transgenic Mice a High-Fat Diet Leads to Overt Diabetes

Thus, an insulin resistance is present but no apparent glucose intolerance (overt diabetes) in the HCV core gene transgenic mice. This is probably because of the genetic background of C57BL/6 mice, which has been shown to maintain either normal or mildly elevated glucose levels despite insulin resistance.[18] To determine whether a high-fat diet exacerbates the prediabetic phenotype, 2-month-old HCV core gene transgenic mice were fed a high-fat diet for up to 8 weeks. Both the transgenic and control mice showed a similar increase (about 30%) in body weight (Figure 4*A*). After 8 weeks on this diet, 100% (10 out of 10) of the transgenic mice exhibited casual (fed) plasma glucose levels >250 mg/dL, whereas none of the 10 control mice fed the same diet exhibited levels >250 mg/dL (325.0 ± 66.6 vs. 179.0 ± 17.4 mg/dL, $P < 0.01$, Figure 4*B*). Insulin levels were significantly higher in the core gene transgenic mice than in control mice both at fasting and fed state (Figure 4*C*, $P < 0.01$ and $P < 0.001$). In control mice, serum insulin levels in high-fat diet state were significantly higher than those in normal diet state at fed state (Figures 1*C* and 4*C*, $P < 0.01$). Although FPG levels were not significantly different between the transgenic and control mice, these results indicate that feeding a high-fat diet leads to the development of overt diabetes in a mouse model for HCV infection. Body weight gain, particularly with high levels of lipid, may trigger the process leading to overt diabetes in an insulin resistance model mouse with compensatory hyperplasia of islet cells.

Insulin Resistance in the Core Gene Transgenic Mice Is Chiefly Caused by Hepatic Insulin Resistance

We then investigated the mechanism of insulin resistance in the core gene transgenic mice. There was no

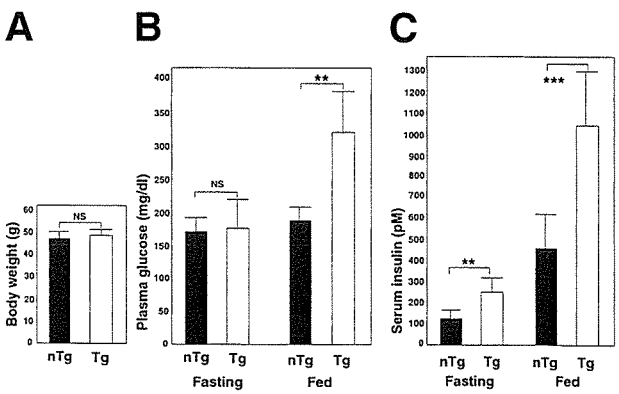

Figure 4. Body weight and glucose homeostasis after a high-fat diet. Control and transgenic mice were fed a high-fat diet for 8 weeks; thereafter, body weight and blood parameters were determined. (*A*) Body weight at the end of the high-fat diet (n = 10 in each group). (*B*) Plasma glucose levels determined in a fasting or fed state (n = 10 in each group). (*C*) Serum insulin levels in a fasting or fed state (n = 10 in each group). Values are mean ± standard error; NS, statistically not significant; $**P < 0.01$; $***P < 0.001$; nTg, nontransgenic mice; Tg, transgenic mice.

significant difference in body weight between the transgenic and control mice as already shown in Figure 1*A*. After the age of 3 months, the core gene transgenic mice developed hepatic steatosis, which is known to be one of the causes of insulin resistance in humans.[19] However, in 1-month-old mouse livers that were used in the analysis of insulin resistance, no hepatic steatosis was noted. No difference was observed in the levels of free fatty acids in the sera between the transgenic and control mice (0.56 ± 0.33 vs. 0.50 ± 0.21 mmol/L, n = 7 in each group, P = 0.65).

Then, we explored the role of the liver in pathogenesis of insulin resistance in the core gene transgenic mice. To directly measure HGP, the hyperinsulinemic-euglycemic clamp technique was conducted as described in Materials and Methods. The core gene transgenic mice showed a normal or slightly lower rate of HGP during the basal period as compared with control mice (Figure 5*A*). Although insulin infusion during the clamp suppressed HGP by 60% in the control mice, insulin induced little effect on HGP of the core gene mice (Figure 5*A*). This is consistent with the notion that insulin resistance in the core gene transgenic mice is chiefly depending on the shortage of insulin action on the liver.

To study the involvement of muscles in the development of insulin resistance in the core gene transgenic mice, we then examined whether or not insulin-stimulated glucose uptake is impaired in the skeletal muscles. The extensor digitorum longus muscle (EDL) from 2-month-old core gene transgenic and control mice were excised and exposed to insulin at the intermediate (0.30 nmol/L) and maximal (10.0 nmol/L) concentrations. There was no significant difference in 2-deoxyglucose uptake in the EDL muscle between the core gene transgenic mice and control mice at either insulin concentration (Figure 5*B*, at 0.30 nmol/L, P = 0.23 and at 10.0 nmol/L, P = 0.76). As another representative muscle that differs from EDL in metabolic properties, the soleus muscle was examined in the same manner as EDL. 2-Deoxyglucose uptake by the soleus muscle was not significantly different between the core gene transgenic and control mice (Figure 5*C*, at 0.30 nmol/L, P = 0.49 and at 10.0 nmol/L, P = 0.49). Thus, in the core gene transgenic mice, contribution of the peripheral skeletal muscle in the development of insulin resistance is negligible. This is in agreement with the observation that the core protein was exclusively present in the liver as detected by Western blotting,[20] which was confirmed by a sensitive enzyme immunoassay (Tsutsumi T. et al., unpublished data, December 2002).[21]

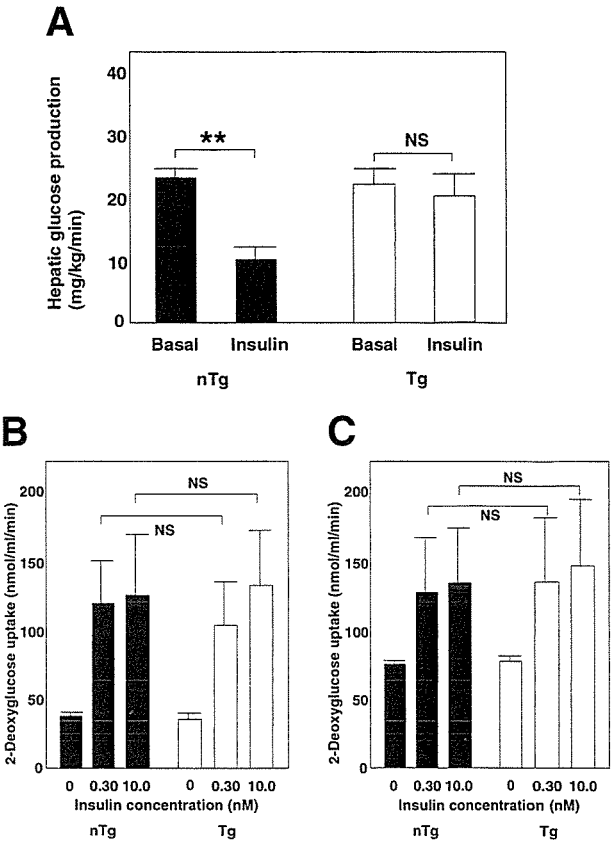

Figure 5. Characterization of glucose metabolism in the core gene transgenic mice. (*A*) Hyperinsulinemic-euglycemic clamp. Hepatic glucose production was calculated using hyperinsulinemic-euglycemic clamp. There was a failure of insulin to suppress hepatic glucose production in the core gene transgenic mice (n = 5 in each group). (*B* and *C*) Glucose uptake by the muscle after insulin stimulation. The extensor digitorum longus muscle (*A*) or soleus muscle (*B*) of 2-month-old mice were excised and exposed to insulin at intermediate (0.30 nmol/L) and maximal (10.0 nmol/L) concentrations. 2-Deoxyglucose uptake was determined as described in the Materials and Methods section (n = 8 in each group). Values are mean ± standard error; NS, statistically not significant; nTg, nontransgenic mice; Tg, transgenic mice.

Elevated TNF-α Level and Altered Tyrosine Phosphorylation of Insulin Receptor Substrate-1 in the Liver and Insulin Resistance

We have noted an increase in TNF-α levels in the liver of HCV core gene transgenic mice,[13] which has also been documented in the sera of human hepatitis C patients.[22–25] On the other hand, TNF-α has been shown to induce insulin resistance in experimental animals and cultured cells.[26–29] Therefore, we next determined the protein expression level of TNF-α by ELISA in the liver of these mice that were used in the current study. The TNF-α levels in the liver of 2-month-old transgenic mice were 702.2 ± 283.3 pg/mg protein and 313.5 ±